

Bacterial Foraging Optimization Based Maximum Power Point Tracking for Photovoltaic System under Partially Shaded Condition with Interleaved Resonant Fly-back Converter

^[1]C Sunil Kumar, ^[2]Dr. Puttamadappa C, ^[3]Dr. Y L Chandrashekar

^[1] Asst. Prof. E&E Engg., PESCE, Mandya, ^[2] Registrar, DSU, Bangalore, ^[3] Prof. & Head MRIT, Mandya

Article Info

Volume 82

Page Number: 15776 - 15784

Publication Issue:

January-February 2020

Article History

Article Received: 18 May 2019

Revised: 14 July 2019

Accepted: 22 December 2019

Publication: 28 February 2020

Abstract:

Due to the non-uniform temperature and irradiance level of PV array, Maximum Power Point Tracking (MPPT) techniques are becoming more common to boost the system efficiency even under varying and unpredictable weather condition. Selection of small value of step size consequence in more convergence for MPPT and large value produces more power oscillations. Therefore, we propose Bacterial Foraging Optimization (BFO-MPPT) algorithm to optimally choose the value of duty cycle that helps to operate the converter at MPP. Moreover, the interleaved converter helps to attain large output power with less ripples and high efficiency. The results prove that the BFO-MPPT can achieve less burden during computation and low computational time with global convergence.

Keywords: Renewable energy, solar system, MPPT, converter, oscillations, micro grid.

I. Introduction

The Renewable Energy System (RES) is growing rapidly around the world in the past decade due to the growing energy demand, especially in growing economies such as China and India with a determined effort to increase energy productivity and carbon emissions reduction [1]. Moreover, the unstable oil pricing and global warming has concerned the world to move towards RES. Out of three renewable sources like geothermal, solar, and biomass that can produce enormous heat energy, solar energy has the highest potential since geothermal sources are only limited to certain locations and biomass is not ubiquitous [2]. However, due to the Partial Shading Condition (PSC) and changing irradiance, tracking the maximum power gains more attention [3]. A converter with Maximum Power Point Tracking (MPPT) placed between the PV system and the load boost the system efficiency when suitable techniques are employed [4].

An effective MPPT technique should require two criteria: (i) the convergence should be quick under varying weather conditions, (ii) the oscillation should be minimum. The MPP techniques can be classified into three classes: conventional techniques, population based, and Artificial Intelligence (AI) methods [5]. The convention techniques that are more commonly used are Incremental Conductance [6], and Perturb and Observe (P&O) [7]. AI techniques include Neural Network (NN) [8] and Fuzzy Logic Controller (FLC) [9]. Population based approaches include Genetic Algorithm [10], Artificial Bee Colony (ABC) [11] etc.

The output of MPPT is generally reference voltage that is given as the input to a controller. The controller in turn produces the duty cycle to operate the Power Converter (PC) which includes buck converter, boost converter, buck-boost converter, SEPIC and so on. The PC employed for MPPT is connected as the input source to the PV module [12].

The remaining paper is structured as follows: section 2 gives the review of the existing approach, section 3 is provided with the illustration of the proposed BFO-MPPT and IRF converter, section 4 provides the simulation setup with performance evaluation, and section 6 gives the conclusion of the paper.

II. Literature Survey

The various techniques that have been proposed to get maximum power from PV system and converter design is reviewed in this section.

Armghanet al. [13] introduced a non-linear control by back stepping for Maximum Power Point Tracking (MPPT) in PV system. They used a single diode PV module to generate power and a non-inverted converter with buck and boost operation to step up or step down the output voltage. The back stepping controller helps to shift the output voltage to the desired MPP by varying the duty cycle. The converter used here has two operating modes and two switches. In the first mode, both the switches are turned on and the load is detached. In the second mode, the switches are turned off and the load is connected. The regression plane provides the reference voltage for the controller and the desired result is obtained by converging the error signal to zero. The tracking performance is tested by varying the irradiance level while maintaining the temperature constant. Although this method obtains MPP further optimization is needed to achieve better results.

Li et al. [14] presented a MPPT algorithm by Improved Gravitational Search Algorithm (IGSA). The active output power is taken as the objective function and the determination of maximum value is considered as the optimization problem. To obtain MPP, the solar current is taken as the fitness of each particle and maximum voltage, maximum current, PV voltage, PV current are the other parameters. To get the MPP, the parameters are first initialized and the initial population is generated. Now, the fitness for each particle or parameters is determined and the value of gravitational constant and mass is updated. After updating the value, the acceleration, velocity,

and total force are calculated. Finally, the position of the particles are updated. When it touches the maximum count of iteration, the desired maximum reference voltage is obtained.

Goudet al. [15] presented a technique to track the maximum power from PV panel under partly shaded state by combining ABC and hill climbing method. Depending upon the shading effect in the P-V curve, either ABC or hill climbing is executed. The proposed system is employed with a current sensor at the terminal of the battery. This sensor detects the shading effect and determine the MPP. The controller detects the duty cycle of the PV array. The steady state of battery current reaches with some delay due to the converter flaws. Therefore, a delay timer is incorporated in the controller. In this, the battery current is measured if the delay timer is true and the corresponding duty cycle is saved.

Eltamaly and Farh [16] used Grey Wolf Optimizer (GWO) with FLC for MPPT in PV system. This combination helps to overcome the disadvantage of both GWO and FLC. The GWO employed at the initial state tracks the MPP quickly and efficiently. The FLC used in the succeeding stage reduces the oscillations. In this method, the initialization of GWO is done based on (i) predefined time (ii) PSC. In predefined initialization, an appropriate time is set based on the frequency of the change in weather. Once the MPP is captured by using GWO, the FLC takes control of tracking until there is variation in irradiance or temperature. The results of MPPT by fuzzy logic GWO proves the reduction of oscillations in the output power.

Tewari et al. [17] introduced a single switch dc-dc converter in PV applications. This converter is developed by combining Switched Inductor (SI), Switched Conductor (SC) and a boost capacitor. The combination of SI and SC helps to attain high voltage gain and the boost capacitor further improves the voltage gain with less stress on the diodes and switch. The principle behind the operation of this converter has two modes: Continuous Conduction Mode (CCM) and Discontinuous Conduction Mode (DCM). CCM can

be further explained in two modes. In mode 1, when the switch is switched on, the energy stored in the switched capacitors is transferred to output capacitor and in parallel, the boost converter and the inductor is charged. In mode 2, when the switch is off, the energy is stored in the boost converter and the inductor is discharged to charge the switched capacitors. The DCM has three modes: The first mode perform the operation similar to that of mode 1 CCM. The operation of mode 2 DCM is again similar to mode 2 CCM but, at the end of the interval the current at the inductor is reduced to zero. In mode 3, the inductor discharges its energy while the switch is turned off.

Teyet al. [18] presented an evolutionary based MPPT algorithm with SEPIC converter under PSC. In this, a type of non-isolated SEPIC converter and MPPT algorithm is used which ensures to get the maximum power from the system. Once the MPP is tracked, controller changes the duty cycle accordingly to the operating point by impedance matching. In this, the impedance is determined by dividing voltage to current. Converter's input impedance represents the impedance of PV array while the converter's load impedance represents the load impedance. To get the PV system operating at MPP, the input impedance is matched with the impedance of MPP. If there is change in load impedance, the input impedance is varied by adjusting the dusty cycle between 0-1.

Basu and Maiti [19], presented a hybrid modular multi-level converter. In this model, DC-link is formed on the basis by the series connection of two sub modules. The sub modules act as a half bridge type which are functioned in terms of pulse width modulation. Then the Low Frequency Converter (LFC) called H-bridge type transforms the resulted DC-link voltage into AC voltage. This structure allows to reach high power level with the minimum number of sub modules. Also, a global MPPT procedure is used to obtain a maximum tracking of power in the PV system. This generate a voltage and current by means of P&O method that allows the current signals to pass through the low pass filter to eradicate unwanted harmonic ripples.

III. PV System model

Temperature and irradiance are given as the input to the PV array from which the maximum power is tracked by using BFO-MPPT algorithm. The duty cycle generated is then used to operate IRF converter. Figure 1 gives the block diagram of the PV system.

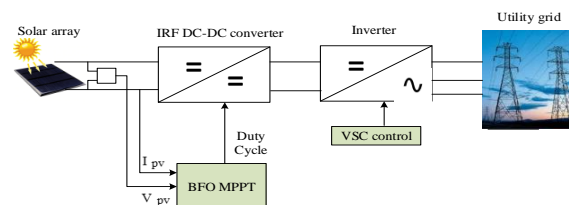


Fig 1: Block diagram for the PV array system

The equivalent circuit of the PV module can be represented as given in Figure 2.

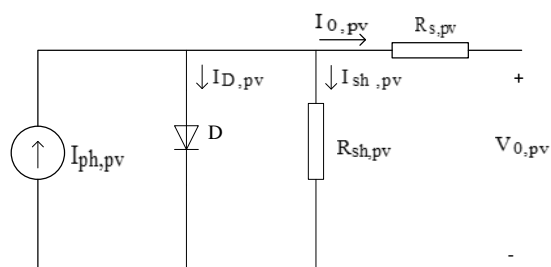


Fig2: Solar cell-single diode model

$$I = I_{ph,pv} - I_{0,pv} \left(\exp \left(\frac{V_{0,pv} + R_{s,pv} I_{0,pv}}{A} - 1 \right) - \frac{V_{0,pv} + R_{s,pv} I_{0,pv}}{R_{sh,pv}} \right) \quad (1)$$

$V_{0,pv}$ and $I_{0,pv}$ are the output voltage and current of the PV cell. $A = \frac{N_s nkT}{q}$

Boltzmann's constant $k = 1.38 \times 10^{-23} J K^{-1}$, charge, $q = 1.602 \times 10^{-19} C$, T denotes the cell temperature, n denotes the ideality factor of diode, N_s denotes the number of series cells.

A. Proposed BFO-MPPT algorithm

BFO is anature inspired algorithm that works based on the foraging strategy of bacteria named E.coli. By using this optimization technique, the MPP in solar system is tracked.

a) *BFO overview*

This algorithm can be explained in four stages. (i) chemotaxis (ii) swarming (iii) reproduction (iv) Elimination & dispersal.

(i) Chemotaxis (local search)

The bacteria movement can be achieved by two ways: swim and tumble. If a bacteria moves towards a location that is rich in nutrients, it continues to swim and when moving towards unfavorable place it tumbles. Here, bacteria denotes the duty cycle and nutrients denotes the MPP i.e. if the duty cycle is moving towards maximum operating point, it swims or else it tumbles. Let K be the entire population of bacteria (duty cycle) with position $P(x, y, z) = \theta_i(x, y, z)$, $i=1,2,\dots,K$ at x^{th} chemotactic, y^{th} reproduction, z^{th} elimination dispersal step. The bacteria movement at chemotaxis stage is given as,

$$\theta_i(x+1, y, z) = D(i) \frac{\Delta(i)}{\sqrt{\Delta(i) \Delta^T(i)}} + \theta_i(x, y, z) \quad (2)$$

Where, $D(i)$ tumble direction of bacteria, Δ denotes the vector in random direction that lie in $[-1,1]$, θ_i denotes the i^{th} value of duty cycle.

(ii) Swarming:

If a bacteria finds the source, it discharges an attractant that helps to gain attention of other bacteria and thus move in groups with high density.

(iii) Reproduction:

Reproduction speeds up the convergence in which, the unhealthy bacteria die and the healthy bacteria divide into two. This helps to maintain the swarm size.

(iv) Elimination and dispersal (Global search)

Sudden change or rise in temperature destroys the swarm of bacteria in the particular area. Therefore, to eliminate the possibility of the bacteria to trap in local search new replacements are initialized randomly in the search space i.e. if the temperature

and irradiance level of the PV system changes, the MPP will transform to a new point. Therefore, θ_i is reinitialized to find the new MPP.

b) *BFO-MPPT procedure*

The execution steps involved in BFO-MPPT are explained as follows.

Step 1: Initialize the duty cycle θ_i , $0.1 < \theta_i \leq 0.9$ with maximum number of iteration $M=25$.

Step 2: Generate five random numbers (tumble direction of bacteria) as initial duty cycle between 0.1 to 0.9 and send them to the DC-DC converter.

Step 3: Fitness evaluation

Compute the fitness function to identify the corresponding best duty cycle $\theta_{i(\text{best})}$ at which the converter operates at MPP, P_{max} by evaluating the fitness function as given in Eqn.(3).

$$f(\theta_i) = P_{\text{cur}}(\theta_i) - P_{\text{max}} \quad (3)$$

$f(\theta_i)$ is the fitness for duty cycle θ_i , $P_{\text{cur}}(\theta_i)$ is the power that is currently generated, P_{max} denotes the maximum power.

If the value of duty cycle (bacteria) is progressing towards MPP (nutrient), the bacteria continues to swim else tumbles.

Step 4: update duty cycle

If $0 < f(\theta_i) \leq 0.5$ local search for nutrients is employed to obtain the next value of duty cycle else performs global search to get the new optimal value of duty cycle.

Step 5: Repeat the steps 3 & 4 until the MPP is reached. Figure 3 illustrates the flow for the BFO-MPPT approach.

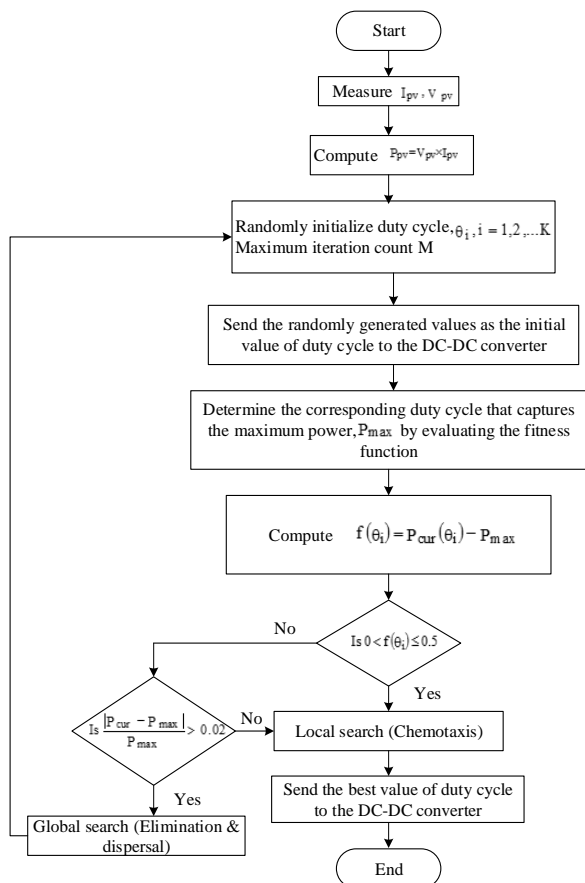


Fig 3: Flowchart for the proposed BF0-MPPT

B. Interleaved Resonant Fly-back (IRF) DC-DC converter

The IRF converter has fly-back converter that consists of a coupled inductor which stores energy during conduction and discharges energy when switched off. The interleaved technique connects the fly-back converters in parallel. Due to this parallel connection, the current gets divided which helps to reduce the current stress, minimizes the loss, and less ripples at the input and the output of the converter. The PWM control technique is widely utilized for switching power supplies. But, PWM has increased switching loss. To overcome this issue, we use resonant converter that achieves Zero Voltage Switching (ZVS) or Zero Current Switching (ZCS). This helps to operate the converter with reduced switching loss and high switching frequency. Figure 4 depicts the circuit diagram for IRF DC-DC converter.

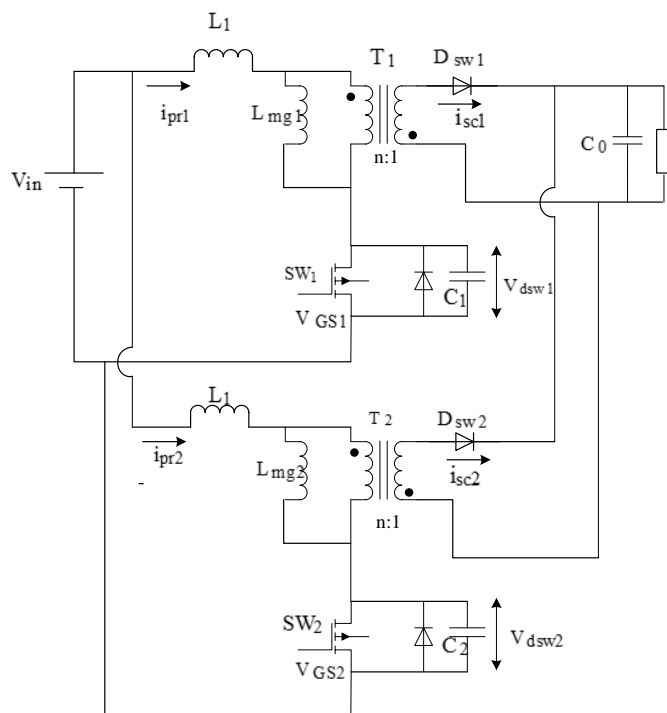


Fig4: Interleaved Resonant Fly back DC-DC converter

Mode 1:

At this mode, the switch SW_1 is turned on and SW_2 is turned off during which the diode D_{sw2} conducts and the diode D_{sw1} is kept in off state. In parallel, the magnetizing inductor L_{mg1} charges and L_{mg2} discharges the energy to the load and the output capacitor C_0 .

$$i_{pr1} = i_{Lmg1} \quad (4)$$

$$i_{sc2} = n i_{Lmg2} \quad (5)$$

$$i_{Lmg1}(t) = (t - t_0) \frac{V_{in}}{L_{mg}} \quad (6)$$

$$i_{Lmg2}(t) = (t - t_1) \frac{nV_o}{L_{mg}} \quad (7)$$

Mode 2:

At this mode, the switch SW_1 is kept on, SW_2 , D_{sw1} , D_{sw2} is turned off. The inductor L_{mg1} charges from the DC source whereas, L_{mg2} is reversely charged by the capacitor C_1 . $L_{mg2} = 0$,

$$V_{dsw2} = nV_o + V_{in} \quad (8)$$

$$f_2 = \frac{1}{2\pi\sqrt{C_2 L_{mg}}} \quad (9)$$

Mode 3:

At this stage, sw_2 is in conduction state and sw_1 , D_{sw1} , D_{sw2} are in non-conduction state. The capacitor C_2 charges from the energy that is discharged from L_{mg1} until $V_{dsw1}=nV_0 + V_{in}$.

$$i_{pr2} = i_{Lmg2} \quad (10)$$

$$i_{Lmg2}(t) = (t - t_3) \frac{V_{in}}{L_{mg}} \quad (11)$$

Mode 4:

In mode 4, SW_1 turned on whereas SW_2 is turned off. During this stage, D_{sw1} conducts and D_{sw2} is kept off. Now, L_{mg2} charges and L_{mg1} releases the stored energy to the load and C_0 via T_1 .

$$i_{sw1} = n i_{Lmg1} \quad (12)$$

$$i_{Lmg1}(t) = -(t - t_4) \frac{nV_0}{L_{mg}} \quad (13)$$

Mode 5:

During this period, SW_1, SW_2, D_{sw2} are turned off and D_{sw1} is turned on. Similar to mode 2, the energy stored in L_{mg1} is discharged to the load and C_0 via T_1 . The capacitor C_2 charges from the energy stored in L_{mg2} until $V_{dsw2} = nV_0 + V_{in}$

Mode 6:

At this time interval, the switches sw_1 and sw_2 are switched off and the diodes D_{sw1}, D_{sw2} conducts. Both the inductor L_{mg1} and L_{mg2} releases the stored energy to the load and C_0 .

$$i_{sw2} = n i_{Lmg2} \quad (14)$$

$$i_{Lmg2}(t) = -(t - t_6) \frac{nV_0}{L_{mg}} \quad (15)$$

Mode 7:

The switches sw_1, sw_2 are turned off during which D_{sw2} conducts and D_{sw1} is turned off. The inductor L_{mg1} is charged reversely by C_1 whereas, the inductor L_{mg2} discharges the energy to the load and C_0 through the transformer T_2 .

$$i_{Lmg1} = 0 \quad (16)$$

$$V_{dsw1} = nV_0 + V_{in} \quad (17)$$

$$f_1 = \frac{1}{2\pi\sqrt{L_{mg}C_1}} \quad (18)$$

IV. Experimental Result & Analysis

To inspect the performance of the BFO-MPPT algorithm with IFR converter, the setup is evaluated on MATLAB/Simulink platform.

A. Simulation Setup

Figure 5 gives the Simulink model for the system. The specification of the PV module used is provided in Table 1.

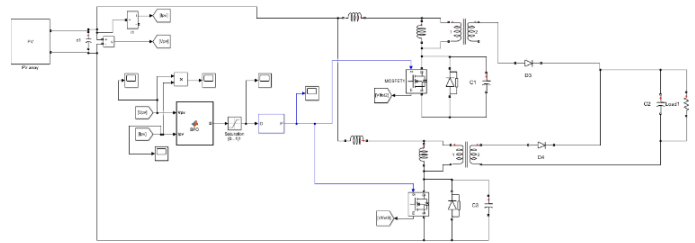


Fig 5: Simulink model for the proposed system

Table 1: Specifications of PV module

Parameter	Value
Temperature	25° C
Irradiance	1000 KW/m2
Maximum power	342.2 W
Current at maximum power	5.9 A
Voltage at maximum power	58 V
Number of population	30
Maximum number of iteration	50

B. Performance Analysis

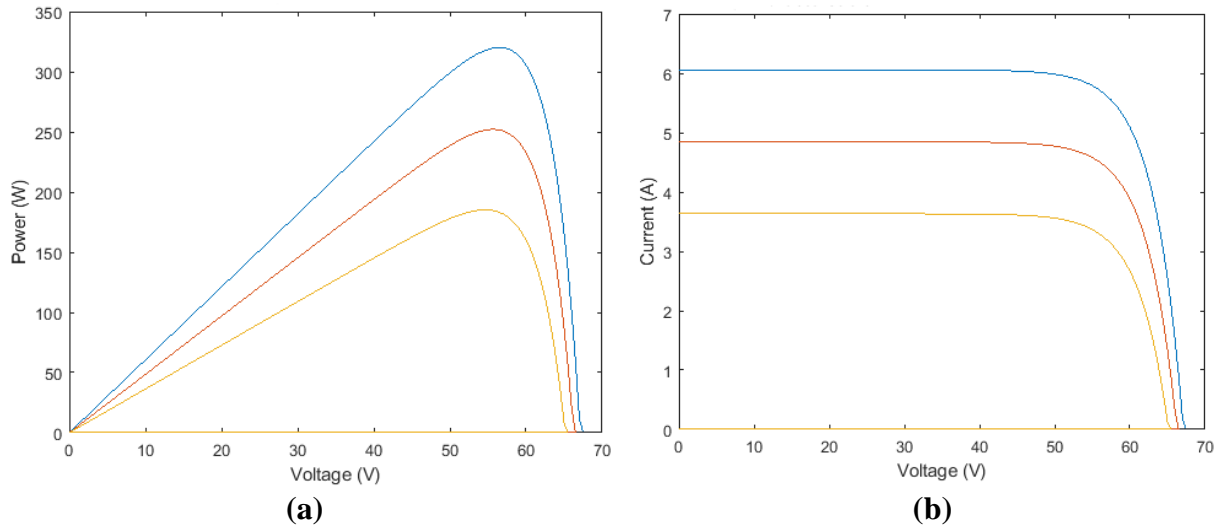
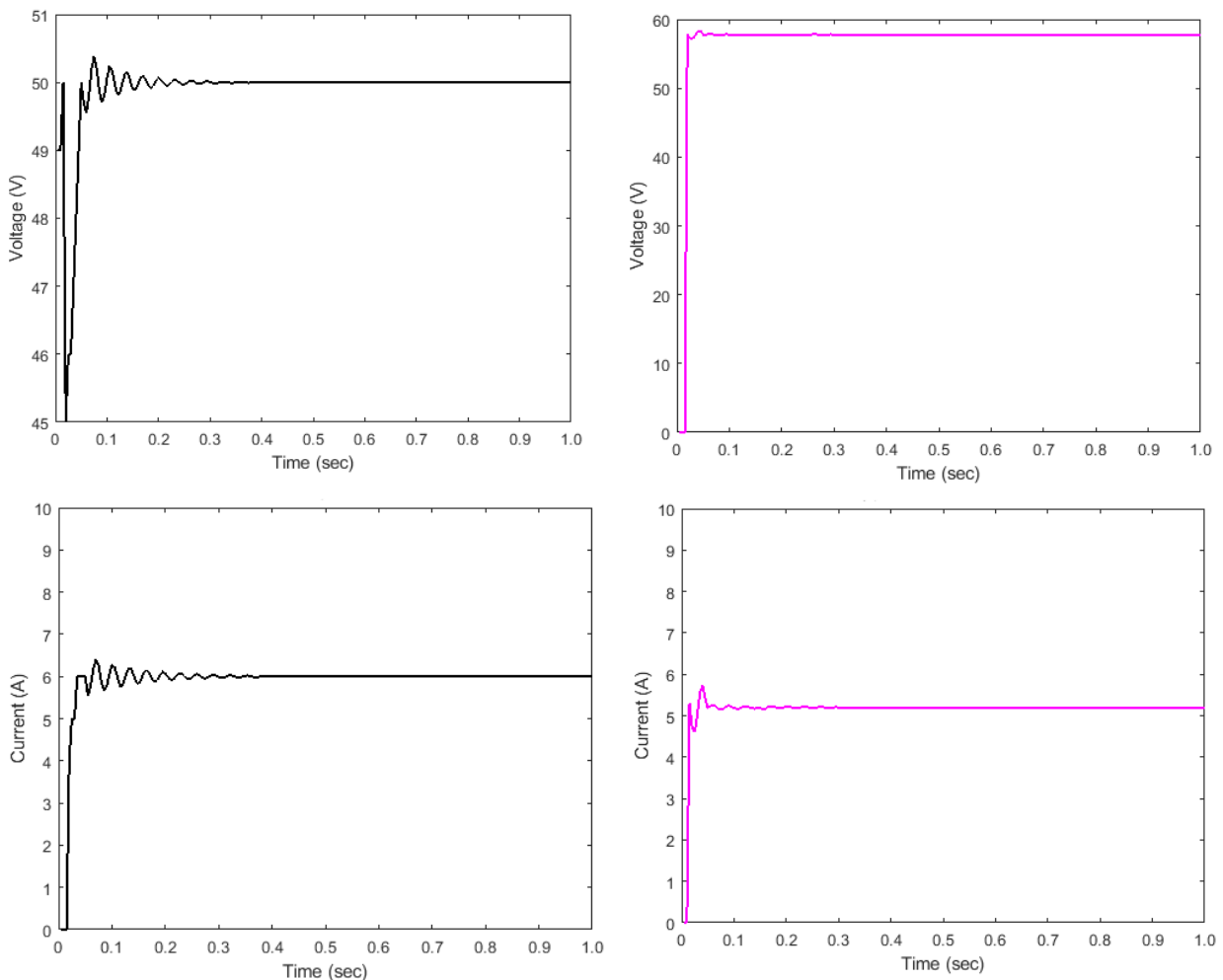


Fig6: Output characteristic curve under varying irradiance (a) P-V curve (b) I-V curve

Figure 6 gives the output P-V and I-V characteristic curve for the PV module under varying temperature. Under high temperature, the system attains the maximum power of 342.2 W. Under this condition, the voltage at maximum power is 58 V and the current at maximum power is 5.9 A. When the

temperature decreases, the power produced also decreases to 267.9 W. During this period, the voltage at maximum power is 57 V and the current at maximum power is 4.7 A.



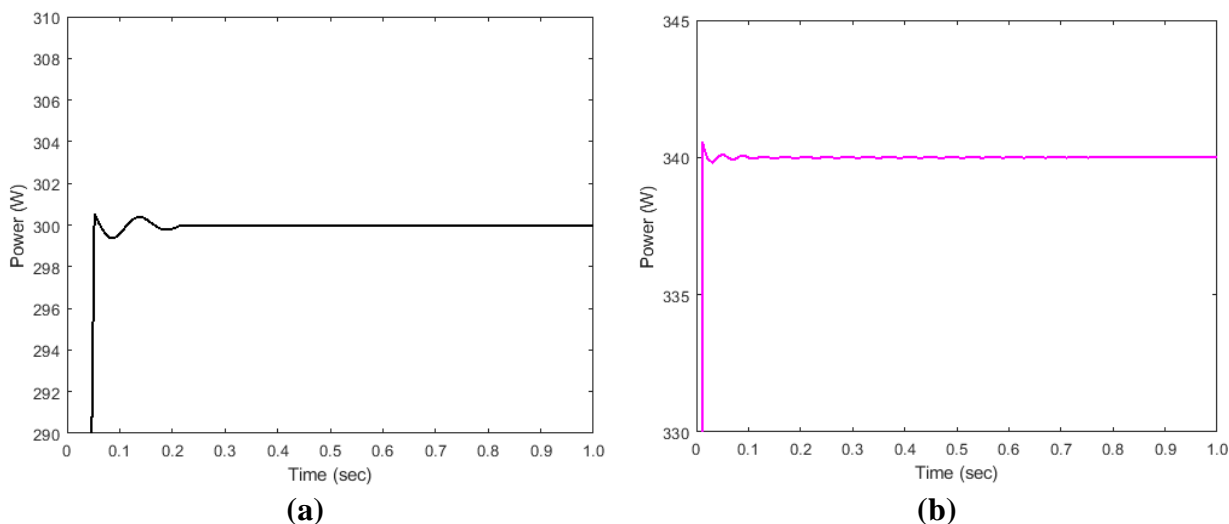


Fig7: Power, current, and voltage curve at high temperature (a) P&O-MPPT (b) BFO-MPPT

Figure 7 (a) gives the Power, current, and voltage curve of P&O technique and Figure 6 (b) shows the performance curve when employing BFO-MPPT algorithm. In this analysis, the settling time, rise time taken for P&O is more than the proposed BFO-MPPT. Moreover, the ripples are more in conventional P&O which in turn increases the overshoot than BFO-MPPT. The improved

performance of proposed MPPT is due to the faster convergence of BFO technique contributing to track the MPP at a faster rate than the conventional method. Also, the use of IRF converter helps to get the maximum output power with less oscillations by the use of interleaved and fly-back technique. Table 2 gives the comparison under different metrics.

Table 2: Performance Comparison

Method/Parameter	Voltage (V_{MPP})	Current (I_{MPP})	Power (W)	Rise time (sec)	Settling time (sec)
P&O MPPT	50	6	300	0.05	0.22
BFO MPPT	54	5.9	342.2	0.01	0.1

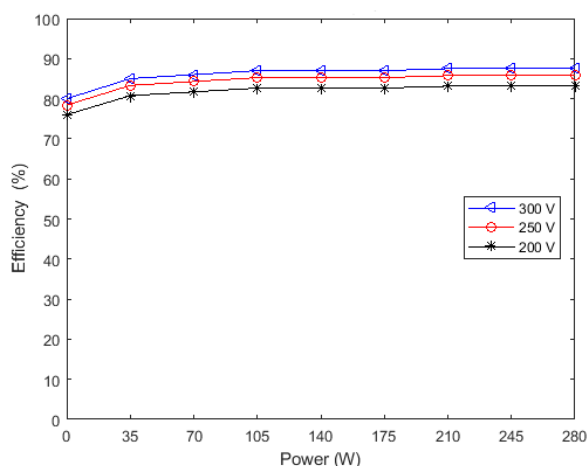


Fig8: Efficiency of system under different output power

Figure 8 shows the efficiency of the system which is obtained by testing under different input voltage. In

this, the IRF converter increases the output power by the parallel connection of fly-back converter and helps to reduce the switching loss and ripples. This reduction in loss and faster tracking improves the efficiency of the system.

V. Conclusion

This paper proposes a BFO-MPPT algorithm with IRF converter. BFO helps to track MPP in the PV system with less oscillation and faster convergence. Initially, the duty cycles are randomly initialized and the fitness for each of the values are determined. Based on the fitness evaluation, the best value of duty cycle that attains MPP is chosen to operate the IFR converter. The IRF converter helps to achieve ZCS/ZVS by the interleaved fly-back technique. The

performance of the BFO-MPPT is evaluated and compared with the conventional P&O algorithm. The evaluation results show that the BFO-MPPT technique has attained higher efficiency and faster tracking response with less ripples, and less loss.

REFERENCES

1. B. Yang, T. Yu, X. Zhang, H. Li, H. Shu, Y. Sang, L. Jiang, "Dynamic leader based collective intelligence for maximum power point tracking of PV systems affected by partial shading condition". *Energy conversion and management*. Vol.179, pp.286-303, 2019
2. E. Kabir, P. Kumar, S. Kumar, A. A. Adelodun, K. H. Kim, "Solar energy: Potential and future prospects". *Renewable and Sustainable Energy Reviews*. Vol.82, pp.894-900, 2018.
3. A. I. Ali, M. A. Sayed, E. E. Mohamed, "Modified efficient perturb and observe maximum power point tracking technique for grid-tied PV system". *International Journal of Electrical Power & Energy Systems*. Vol.99, pp. 192-202, 2018.
4. S. Xiao, R. S. Balog, "An improved adaptive perturb & observe maximum power point tracking technique". In 2018 IEEE Texas Power and Energy Conference (TPEC), IEEE, pp. 1-6, 2018.
5. H. Armghan, I. Ahmad, A. Armghan, S. Khan, M. Arsalan, "Backstepping based non-linear control for maximum power point tracking in photovoltaic system". *Solar Energy*. vol. 159, pp. 134-41, 2018.
6. K. S. Tey, "Mekhilef Modified incremental conductance MPPT algorithm to mitigate inaccurate responses under fast-changing solar irradiation level". *Solar Energy*. vol.101, pp. 333-42, 2014.
7. V. K. Devi, K. Premkumar, A. B. Beevi, S. Ramaiyer, "A modified Perturb & Observe MPPT technique to tackle steady state and rapidly varying atmospheric conditions". *Solar Energy*, vol.157, pp.419-26, 2017.
8. F. Dkhichi, B. Oukarfi, Y. El Kouari, Ouoba D, "A. Fakkar Neural network based integration of MPPT and diagnosis of degradation for photovoltaic module". *Optical and Quantum Electronics*. Vol.48, no.2, pp.105, 2016.
9. Y. T. Chen, Y. C. Jhang, R. H. Liang. A fuzzy-logic based auto-scaling variable step-size MPPT method for PV systems. *Solar Energy*, vol.126, pp. 53-63, 2016.
10. A. Badis, M. N. Mansouri, M. H. Boujmil "A genetic algorithm optimized MPPT controller for a PV system with DC-DC boost converter". In 2017 International Conference on Engineering & MIS (ICEMIS), IEEE, pp. 1-6, 2017.
11. D. Pilakkat, S. Kanthalakshmi An improved P&O algorithm integrated with artificial bee colony for photovoltaic systems under partial shading conditions. *Solar Energy*. Vol.178, pp.37-47, 2019.
12. R. Ayop, C. W. Tan Design of boost converter based on maximum power point resistance for photovoltaic applications. *Solar Energy*, vol.160, pp.322-35, 2018.
13. H. Armghan, I. Ahmad, A. Armghan, S. Khan, M. Arsalan Backstepping based non-linear control for maximum power point tracking in photovoltaic system. *Solar Energy*. Vol.159, pp. 134-41, 2018.
14. L. L. Li, G. Q. Lin, M. L. Tseng, K. Tan, M. K. Lim. A maximum power point tracking method for PV system with improved gravitational search algorithm. *Applied Soft Computing*. vol.65, pp.333-48, 2018.
15. J. S. Goud, R. Kalpana, B. Singh. "A Hybrid Global Maximum Power Point Tracking Technique With Fast Convergence Speed for Partial-Shaded PV Systems". *IEEE Transactions on Industry Applications*. Vol.54, no.5, pp.5367-76, 2018.
16. A. M. Eltamaly, H. M. Farh. "Dynamic global maximum power point tracking of the PV systems under variant partial shading using hybrid GWO-FLC". *Solar Energy*. Vol.177, pp.306-16, 2019.
17. N. Tewari, V. T. Sreedevi, "A novel single switch dc-dc converter with high voltage gain capability for solar PV based power generation systems". *Solar Energy*, vol.171, pp.466-77, 2018.
18. K. S. Tey, S. Mekhilef, M. Seyedmahmoudian, B. Horan, A. T. Oo, A. Stojcevski, "Improved differential evolution-based MPPT algorithm using SEPIC for PV systems under partial shading conditions and load variation". *IEEE Transactions on Industrial Informatics*. Vol.14, no.10, pp.4322-33, 2018
19. T. S. Basu, S. Maiti "A hybrid modular multilevel converter for solar power integration". *IEEE Transactions on Industry Applications*. Vol.55, no.5, pp.5166-77, 2019.